CORTEX 65 (2015) 219–231

Available online at www.sciencedirect.com

ScienceDirect

Journal homepage: www.elsevier.com/locate/cortex

Research report

Fronto-insula network activity explains emotional dysfunctions in juvenile myoclonic epilepsy: Combined evidence from pupillometry and fMRI

Frieder Michel Paulus [a,b,*,1], Sören Krach [a,*,1], Marius Blanke [c], Christine Roth [d], Marcus Belke [d], Jens Sommer [e], Laura Müller-Pinzler [a,b], Katja Menzler [d], Andreas Jansen [e], Felix Rosenow [b,g], Frank Bremmer [c], Wolfgang Einhäuser [c,f,1] and Susanne Knake [d,1]

[a] Department of Psychiatry and Psychotherapy, Social Neuroscience Lab, University of Lübeck, Lübeck, Germany
[b] Department of Child- and Adolescent Psychiatry, University of Marburg, Marburg, Germany
[c] Department of Neurophysics, University of Marburg, Marburg, Germany
[d] Department of Neurology, University of Marburg, Marburg, Germany
[e] Section of Brainimaging, Department of Psychiatry and Psychotherapy, University of Marburg, Germany
[f] Center for Interdisciplinary Research (ZiF), Bielefeld, Germany
[g] Epilepsy Center Frankfurt Rhine-Main, Department of Neurology, Center of Neurology and Neurosurgery, Goethe-University, Frankfurt a. M., Germany

ARTICLE INFO

Article history:
Received 20 June 2014
Reviewed 1 September 2014
Revised 31 October 2014
Accepted 27 January 2015
Action editor Gus Buchtel
Published online 7 February 2015

Keywords:
Juvenile myoclonic epilepsy
fMRI
Pupillometry
Anterior cingulate cortex
Empathy
Emotion

ABSTRACT

Emotional instability, difficulties in social adjustment, and disinhibited behavior are the most common symptoms of the psychiatric comorbidities in juvenile myoclonic epilepsy (JME). This psychopathology has been associated with dysfunctions of mesial-frontal brain circuits. The present work is a first direct test of this link and adapted a paradigm for probing frontal circuits during empathy for pain. Neural and psychophysiological parameters of pain empathy were assessed by combining functional magnetic resonance imaging (fMRI) with simultaneous pupillometry in 15 JME patients and 15 matched healthy controls. In JME patients, we observed reduced neural activation of the anterior cingulate cortex (ACC), the anterior insula (AI), and the ventrolateral prefrontal cortex (VLPFC). This modulation was paralleled by reduced pupil dilation during empathy for pain in patients. At the same time, pupil dilation was positively related to neural activity of the ACC, AI, and VLPFC. In JME patients, the ACC additionally showed reduced functional connectivity with the primary and secondary somatosensory cortex, areas fundamentally implicated in processing the somatic cause of another's pain. Our results provide first evidence that alterations of mesial-frontal circuits directly affect psychosocial functioning in JME patients and draw a link of pupil dynamics with brain activity during emotional processing. The findings of reduced pain empathy related activation of the ACC and AI and aberrant functional integration of the ACC with somatosensory cortex areas provide further

* *Corresponding authors*. Department of Psychiatry, Social Neuroscience Lab, University of Lübeck, Ratzeburger Allee 160, 23538 Lübeck, Germany.
E-mail addresses: paulus@snl.uni-luebeck.de (F.M. Paulus), krach@snl.uni-luebeck.de (S. Krach).
[1] These authors contributed equally to this work.
http://dx.doi.org/10.1016/j.cortex.2015.01.018

evidence for this network's role in social behavior and helps explaining the JME psychopathology and patients' difficulties in social adjustment.

1. Introduction

The ability to share another person's feelings is a prerequisite for adequate social adjustment and psychosocial behavior (Davis, 1996). The neurobiology of such empathic processes is explained by shared representations of one's own and another's affect in similar neural networks. Particularly the activation of a mesial fronto-insular network including the anterior cingulate cortex (ACC) and the anterior insula (AI), as well as somatosensory areas are thought to constitute the neural pathways for sharing another's feelings (Keysers, Kaas, & Gazzola, 2010). In this line, recent investigations linked the response of this network to motivating interpersonal behavior in healthy participants (Hein, Silani, Preuschoff, Batson, & Singer, 2010) and to disorders such as autism or psychopathy which are characterized by fundamental impairments in psychosocial behavior (Meffert, Gazzola, den Boer, Bartels, & Keysers, 2013; Silani et al., 2008).

Emotional instability, social inadequacy, disinhibition and difficulties in social adjustment are the most frequent psychiatric comorbidities of juvenile myoclonic epilepsy (JME), a frequent idiopathic form of generalized epilepsy (Janz, 1985; Janz & Christian, 1957). On an anatomical level, early autopsy studies by Meencke and Janz (1984) as well as Meencke (1985) have found microscopic malformations including atypical cells and abnormal cortical architecture ("microdysgenesis") post-mortem in about 4% of healthy adults and 18% of children. In contrast, microdysgenesis was found in 37% of patients with epilepsies and in 87% of patients with generalized epilepsies. They suggested that such microdysgenesis might be a marker of early developmental damage (for a critical reflection on the significance of the histological findings reported by Meencke and Janz see Lyon & Gastaut, 1985). These histological results motivated more recent analyses on a rather macroscopic scale with non-invasive imaging such diffusion tensor imaging (DTI), magnetic resonance imaging (MRI) and magnetic resonance spectroscopy. Voxel-based morphology (Betting et al., 2006; Kim et al., 2007; Woermann, Free, Koepp, Sisodiya, & Duncan, 1999) and magnetic resonance spectroscopy studies (Savic, Lekvall, Greitz, & Helms, 2000) have now repeatedly found local structural abnormalities in the mesial-frontal lobe of JME patients that could explain the peculiarities in the personality structure and frequent comorbidities of JME with psychiatric conditions (Gelisse, Thomas, Samuelian, & Gentin, 2007). More recently, these findings were complemented by connectivity analyses using DTI, functional MRI (fMRI) and electroencephalography (EEG). Besides atypical integration of the anterior supplementary motor area (SMA, Vollmar et al., 2011; Vulliemoz et al., 2011), these studies additionally revealed alterations in functional and anatomical connections in more ventral aspects of the mesial-frontal lobe including the ACC, via fronto-thalamic (Deppe et al., 2008; Holmes, Quiring, & Tucker, 2010; O'Muircheartaigh et al., 2012), transcallosal (O'Muircheartaigh et al., 2011), and pre-SMA (Vollmar et al., 2012) connections. Despite the evident overlap of these structural disturbances with networks that regulate interpersonal behavior, no functional neuroimaging study has yet directly examined how alterations in frontal circuit functioning may contribute to patients' difficulties in socio-emotional adjustment.

We combined pupillometry and fMRI to investigate frontal lobe functioning in response to others' bodily pain as an indicator for empathic responding in JME patients and healthy controls. Since the pupil responds to various neurocognitive processes (Steinhauer, Siegle, Condray, & Pless, 2004), and characteristically dilates during negative emotions (Bradley, Miccoli, Escrig, & Lang, 2008; Janisse, 1974; Partala & Surakka, 2003) pupillometry provides an outwardly observable measure of brain reactivity to emotional stimuli (Silk et al., 2007). In this line, a recent study could demonstrate that the pupil also dilates during the experience of pain. Importantly, the magnitude of the pupil dilation was thereby well predictive of the intensity of the pain subjects experienced (Geuter, Gamer, Onat, & Büchel, 2014). Hence, the pupil's response may also help to objectify the experienced empathy for others' bodily pain beyond the mere self-report measure. Specifically, we hypothesized that (i) the empathy-related mesial-frontal circuit activation is diminished in patients with JME, (ii) pupil dilation in response to others' pain accordingly is affected in JME, (iii) pupil dilation is significantly coupled with arousal-related neural activation, and (iv) differences in neural activation relate to altered connectivity of the mesial fronto-insular network.

2. Methods

The study was approved by the ethics committee at the Faculty of Medicine, University Marburg (AZ 46/10). All participants provided written informed consent.

2.1. Sample characteristics

Fifteen individuals with JME (10 females, mean age = 34.3, *SD* = 12.7 years, Table 1) and 15 controls (10 females, mean age = 32.5, *SD* = 12.9 years) with no history of psychiatric or neurologic conditions participated in the combined fMRI-pupillometry study. Healthy controls (HCs) were matched with respect to age, sex, handedness, and verbal IQ. The rationale for matching for verbal IQ was ensuring similar levels of conceptual understanding of the instructions and experimental paradigm. Patients were recruited at the local tertiary epilepsy center. All were taking antiepileptic medication and were seizure-free for generalized tonic-clonic

Table 1 – Sample characteristics.

	JME	Controls	*p*
Age (years)	30.3 ± 11 (30 ± 11)	29.9 ± 12.1 (28.8 ± 11.2)	.925 (.784)
Sex ratio (f/m)	10/5 (9/3)	10/5 (9/4)	1 (.748)
Handedness	65.6 ± 37.6 (71.8 ± 24.1)	56.3 ± 35.4 (55.1 ± 36.7)	.493 (.197)
Verbal IQ	107.8 ± 12.4 (106.7 ± 12.8)	116.3 ± 13.1 (115.1 ± 13.5)	.079 (.124)
Education (years)	11.67 ± 1.4 (11.83 ± 1.4)	12.4 ± 1.2 (12.5 ± 1.1)	.150 (.178)

Note. Handedness was assessed with the Edinburgh handedness inventory. Verbal IQ was assessed using the German Mehrfachwahl Wortschatz Test Version B. Numbers in parentheses indicate frequencies or means and standard deviations for the sub-group of participants for which valid eye-tracking data was available. *p*-values result from two-sample *t*-tests for mean differences or chi-square tests for differences in frequencies.

seizures for at least 6 months (Table 2). One patient had occasional myoclonic seizures. The mean age at epilepsy onset was 14.3 years ($SD = 3.2$) the average disease duration at the time of fMRI data acquisition was 14.9 years ($SD = 11.5$). All participants had normal or corrected-to-normal vision.

Notably, the sample of JME patients for the combined fMRI-pupillometry study was a subset of a larger sample of JME patients who participated in an ongoing structural MRI and DTI study. Within the full sample of $N = 19$ JME patients and $N = 20$ matched HCs we also explored whether JME patients showed signs for increased levels of alexithymia. Broadly, the construct of alexithymia conceptualizes the inability to identify and describe one's own emotions as a stable personality characteristics (Taylor, 1984; Taylor, Michael Bagby, & Parker, 1991) that is related to various psychiatric conditions (Cox, Swinson, Shulman, & Bourdeau, 1995). It is not unlikely that alexithymic traits are also elevated in JME patients since frontal lobe functioning has strong implications in the understanding and regulation of one's own emotions (Berthoz et al., 2002; Damasio et al., 2000; Eippert et al., 2007). To explore the association of JME with alexithymia, we administered the Toronto Alexithymia Scale (TAS), a 20-item questionnaire that assesses the ability to understand, describe and process one's own emotions. Overall, the internal consistencies of the TAS total score and sub-scales in the present sample were good and in the range of previous literature (Parker, Taylor, & Bagby, 2003) with all Cronbach's alphas exceeding .72.

2.2. *Functional MRI paradigm*

Fifty-six digital color photographs depicting another person's hand or foot from a first-person perspective were selected from a previously described stimulus set (Jackson, Meltzoff, & Decety, 2005). Half of the images (28) depicted a painful situation ('Pain'), the other half ('Neutral') depicted a similar non-painful situation. Important for the pupillometric analysis, luminance did not differ between painful and neutral stimuli [$t(27) = .26$, $p = .79$]. Images were presented in pseudo-randomized order on an LCD screen (12.2 by 9.3° visual angle) using Presentation 11.0 (Neurobehavioral Systems, Albany, CA, USA). Participants viewed each image for 4.5 sec, followed by a blank screen (1.5 sec), rating period (3 sec), and a jittered baseline (average = 6.1 sec, see Fig. 1A), totaling 15.4 min per experiment. Aided by two example photographs not used in the actual experiment, participants were instructed to estimate the intensity of the pain that the person feels in the depicted situation on a 5-point Likert scale (from 1 = "not at all" to 5 = "very strongly"). During the MRI participants gave the rating responses with a button press of the right hand fingers.

Table 2 – JME patient characteristics and medication.

Patient ID	Pupil	Sex	Age	Age at onset	IQ	Medication, in *mg/day*			
						Lamotrigine	Levetiracetame	Valproate	Carbamazepine
JME_012		m	33	17	124	50	2000	1250	
JME_013	x	m	24	11	93			1,800	
JME_014	x	f	29	11	95		3000		
JME_015		m	44	14	112		4000	3000	800
JME_016		f	18	16	101	200		800	
JME_018	x	f	52	14	130		3750	1500	
JME_019	x	m	23	19	118			600	
JME_021	x	f	24	13	112	200			
JME_024	x	f	52	12	112			450	
JME_028	x	m	34	18	124		2000		
JME_031	x	f	25	18	107	250			
JME_037	x	f	24	15	92	400			
JME_041	x	f	31	13	104			1500	
JME_042	x	f	22	16	100		1000		
JME_046	x	f	20	7	93			900	

Note. A cross in the 'pupil' column indicates that valid eye-tracking data were available for the respective patient.

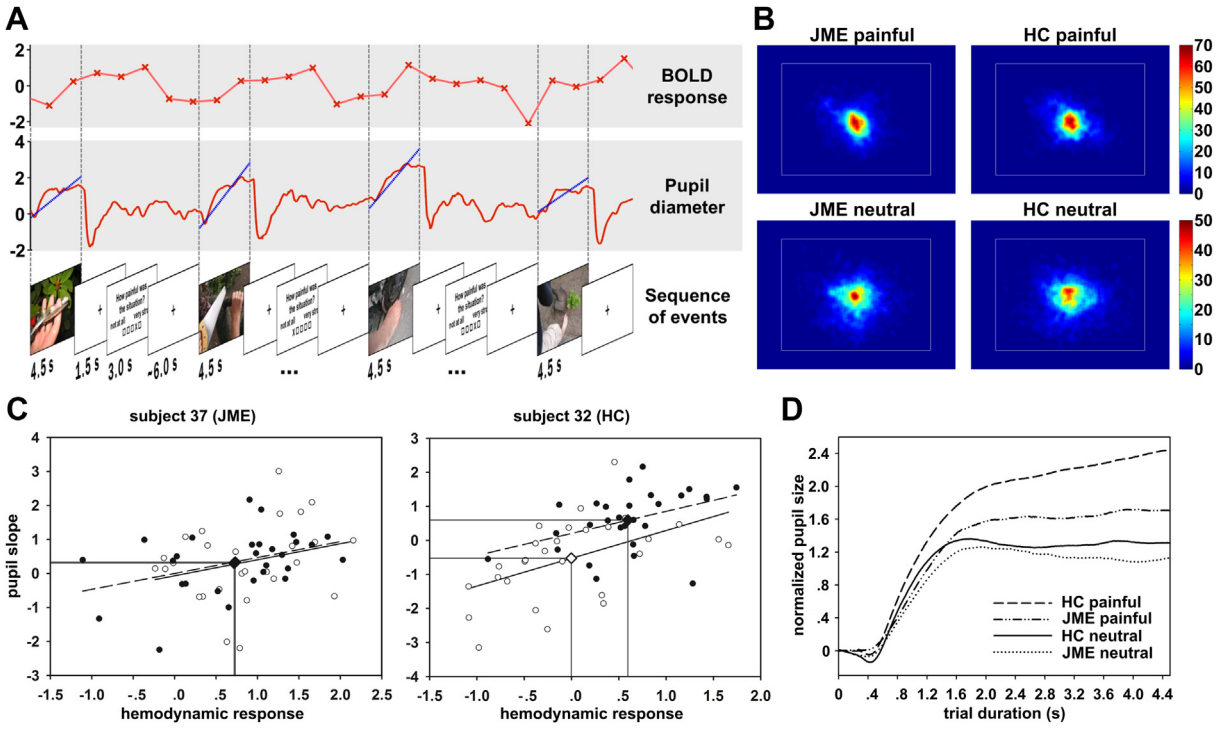

Fig. 1 – Gaze directions, pupil dilation and integration of pupillometry with hemodynamics. A Sequence of the experimental paradigm and multi-modal-dependent variables. *Bottom row*: Experimental paradigm to induce empathic pain in the observers. The trial structure is exemplified with pictures showing painful or neutral, non-painful situations together with the subsequent rating period and low-level baseline (fixation cross). *Middle row, red*: z-normalized trace of the pupil diameter for one subject; for visualization periods of blinks were interpolated using cubic-spline interpolation; *blue*: a trial-specific 'pupil slope' is computed as optimal linear regression in the least-squares sense on the pupil signal during the time of stimulus presentation. These trial-specific pupil slopes were entered into the hemodynamic model in order to identify common variance in the blood oxygen level dependent (BOLD) signal (*top row*) and the pupil trace. B Heatmaps of the gaze direction in both groups for each stimulus condition. Gaze patterns of healthy controls (HC) are depicted in the right column and those of patients with juvenile myoclonic epilepsy (JME) in the left column. The size of the maps corresponds to the full screen (800 × 600 pixels, 16.5 × 12.5° of visual angle) and white rectangles indicate the size of the images that were presented on the screen (600 × 450 pixels, 12.5 × 9.4°). Maps were smoothed with a 20 pixel-wide (.4°) square kernel for displaying purposes. Colorbars indicate absolute number of samples per bin; colormaps are identical within each row (i.e., for the same condition between groups), but differ between rows (i.e., between conditions). C Association of the hemodynamic response in the right anterior cingulate cortex (ACC) with sustained pupil dilation while watching another's limb in painful and neutral conditions. The example on the within-subject level illustrates how the observed effects in pupil dilation relate to neural activation in the group of JME patients and healthy controls. Scatter plots show single trial estimates of the hemodynamic response in the right ACC at 8, 22, 40 mm and the slope of the pupil dilation for single subjects (*left*: patient, *right*: sex matched HC) in artificial numbers (i.e., β-values). Black dots indicate estimates of the hemodynamic response and the slope of the pupil dilation in the painful condition, white dots in the neutral condition. Accordingly, black and white diamonds represent the averaged responses within conditions across trials. Slopes illustrate the positive association with a least-square fit of a linear regression within the painful condition (dashed, subject 37 Pearson's $r = .42$ and subject 32 $r = .42$) and the neutral condition (solid, subject 37 $r = .27$ and subject 32 $r = .51$). Consistent with the group-level analysis, the pupil slope is positively associated with the hemodynamic signal in the ACC, regardless of the condition. Yet, the mean level of both the hemodynamic response and the pupil slope increased while observing painful stimuli of another's limbs in the control participant only. D Average dilation of the pupil during the presentation of painful or neutral stimuli for both groups. For this illustration, blink-interpolated and normalized pupil traces (see panel A, middle row) were centered on each trial onset and condition averaged for each subject.

2.3. *Functional MRI data acquisition and preprocessing*

Participants were scanned at 3T (Tim TRIO, Siemens Medical Solutions, Erlangen, Germany) with 36 near-axial slices and a distance factor of 10% providing whole-brain coverage. An echo planar imaging (EPI) sequence was used for acquisition of 395 functional volumes during the experiment (TR: 2.2 sec, TE: 30 msec, flip angle: 90°, slice thickness: 3 mm, FoV: 192).

fMRI data were analyzed using SPM8 (www.fil.ion.ucl.ac.uk/spm). After removing the first eight volumes of the time

series the remaining 387 EPI volumes were slice-timed, motion-corrected, and spatially normalized to the standard EPI-template of the Montreal Neurological Institute (MNI). The normalized volumes were re-sliced with a voxel size of 2 × 2 × 2 mm, smoothed with an 8 mm full-width half-maximum isotropic Gaussian kernel, and high-pass filtered at 1/192 Hz.

2.4. *Pupillometry and gaze behavior*

Throughout fMRI acquisition, pupil diameter was recorded monocularly at 500 Hz using a non-invasive MRI-compatible Eyelink-1000 eye-tracking device (SR Research, Kanata, ON, Canada). Valid eye-tracking data was obtained for 12 of the JME patients (9 female, mean age = 30, *SD* = 11 years) and 13 controls (9 female, mean age = 28.8, *SD* = 11.2 years). For each image presentation, the slope of the pupil trace ('pupil slope', Fig. 1A), computed as optimal linear regression in the least-squares sense on the pupil signal during the time of the stimulus presentation, provided a trial-specific measure of the pupil dilation (Stoll et al., 2013). The so derived measure showed excellent reliability for the painful (Cronbach's $\alpha = .90$) as well as the non-painful condition ($\alpha = .86$) and was further used for quantitative analyses: (i) to test the association of sustained pupil dilation with the hemodynamic signal the 'pupil slope' was included as parametric regressor in the fMRI model (see below) and (ii) to test the condition and group effects on the 'pupil slope' in a 2 × 2 repeated measures ANOVA.

To quantify whether gaze behavior differed in terms of fixated image locations or fixation durations, we determined periods of fixations using the built-in algorithm of the Eyelink device with default settings (saccade thresholds: 35 deg/sec for velocity, 9500 deg/sec^2 for acceleration). For illustration purposes, we in addition use the complete gaze data sampled at 500 Hz (Fig. 1B).

2.5. *fMRI data analyses*

2.5.1. *Empathy for pain related neural activation and association with pupil dilation*

Two separate fixed-effects general linear models (GLMs) were calculated on the within-subject-level. These included three epoch regressors each modeling the hemodynamic responses to the painful situations, neutral situations, or the rating period. Head-movement parameters were included to control for noise. The first GLM was implemented to test for activation differences between the JME and control group. Here, a parametric modulator coded the trial-specific intensity rating for the painful pictures. Weighted β-images contrasting the painful to the neutral condition were computed and analyzed at the group level. The second GLM tested the association of the pupil dilation with the hemodynamic response (Fig. 1A). Therefore, the trial specific pupil dilation was entered as an additional parametric weight for the corresponding neutral and painful picture in the subsample of $N = 25$ participants for whom valid eye-tracking data was available. β-images of the parametric modulators of the pupil dilation during the painful and neutral condition were analyzed at the group level.

Two separate random-effects GLMs were computed at the group-level. The first model compared the empathy for pain-related neural activation in the JME and the healthy control group. The second model tested the association of trial-by-trial variability in the pupil slope and the hemodynamic response with a 2 × 2 repeated measures design including the parametric weights of the 'pupil slope' within the neutral and painful conditions and the JME and control groups. To control for potential confounds due to group differences in pupil dynamics, this model included the intra-individual standard deviations of the 'pupil slope' as covariates for each group (cf. Fig. 1C).

To estimate trial-specific responses of the ACC for single participants, time series were extracted as the first eigenvariate of a spherical region of interest (ROI) with a radius of 4 mm. Time series were high-pass filtered with 1/192 Hz, mean centered, and adjusted for movement-related artifacts and hemodynamic responses induced by the rating period with an effects-of-interest correction. Trial-specific hemodynamic responses were then estimated with the above-described stimulus durations of 4.5 sec using MarsBaR v 0.43 (Brett, Anton, Valabregue, & Jean-Baptiste, 2002).

2.5.2. *Functional connectivity analysis of the ACC*

For the analysis of functional connectivity, we applied a seed region approach comparable to procedures described previously for functional connectivity analyses during task execution (Paulus et al., 2013; Paulus, Bedenbender, et al., 2014). The left and right ACC were selected as the seed regions. In order to determine seed voxels located within the ACC, we constrained the search space to the task-activated regions in the ACC within either the left or right hemisphere. For each participant the signal was extracted within these masks at the maximum effect for the contrast comparing the hemodynamic response to the painful and neutral pictures. Neural signal was extracted as the first eigenvariate in a sphere of 4 mm radius as implemented in SPM8 and task-related variance was removed by applying an effects-of-interest correction with an *F*-contrast set on the six movement parameters. To account for noise, three additional time-series were extracted for each subject from the first eigenvariates of all voxels within masks covering medial cerebrospinal fluid (CSF) or left or right hemispheric white matter (Esslinger et al., 2009).

The fixed-effects GLM on the subject-level included the extracted seed time series of the left or right ACC, the left and right WM noise regressors and the CSF noise regressor. Additionally, the functional connectivity models included the three epoch regressors modeling the hemodynamic responses to the painful situations, neutral situations, or the rating period, the corresponding parametric modulators as well as head-movement parameters. ß-maps of the left or right ACC seed time series were analyzed at the group-level using two-sample *t*-tests.

All results were corrected for multiple-comparisons using Gaussian-random field theory as implemented in SPM8 and overlap between neural activation and cytoarchitectonic areas was tested with the SPM ANATOMY toolbox v1.8 if available (Eickhoff et al., 2005). Brain imaging results were visualized using Caret (Van Essen et al., 2001) and the BrainNet Viewer (Xia, Wang, & He, 2013).

3. Results

3.1. Association with alexithymia

Patients with JME showed slightly elevated TAS scores. We found a trend towards increased trait levels of alexithymia for the TAS total score [$t(28) = 1.47$, $p = .076$, $M_{JME} = 46.54$, $SD = 12.93$, $M_{HC} = 40.87$, $SD = 7.53$, $d = .55$] and the facet difficulties to identify emotions [$t(28) = 1.54$, $p = .067$, $d = .56$]. This sample included five patients who were above the cut-off (≥52) and only one participant out of the control group, that might indicate a clinically relevant characteristic [$\chi^2(1) = 3.33$, $p = .068$]. Notably, this effect was statistically significant in the unrestricted sample, including all assessed patients regardless of whether they participated in the combined fMRI-pupillometry study: patients scored higher on the TAS-20 [$t(37) = 1.9$, $p = .032$, $M_{JME} = 46.83$, $SD = 11.63$, $M_{HC} = 40.70$, $SD = 8.08$] with most prominent differences in the facet 'difficulties to identify emotions' [$t(37) = 2.14$, $p = .018$]. The increased levels of alexithymia would have indicated a clinically relevant characteristics in 6 out of the 19 JME patients and 2 out of 20 HCs [$\chi^2(1) = 2.79$, $p = .095$].

3.2. Behavioral data

Overall, response rates during the fMRI experiment were near ceiling. Average response rates were 99.7% for the control group (min = 98%) and 99.3% for the JME group (min = 96%). Reaction times and pain-intensity ratings each showed a significant main effect of condition [$Fs(1,28) > 47.56$, $ps < .001$, $\eta^2 > .63$, rmANOVA]. Post-hoc comparisons indicated intensity ratings to be stronger for painful ($M = 4.03$, $SD = .41$) than for neutral pictures ($M = 1.10$, $SD = .10$) and response times to increase accordingly [$M_{painful} = 893$ msec, $SD = 238$ msec and $M_{neutral} = 666$ msec, $SD = 133$ msec, respectively, $ts(29) > 6.91$, $ps < .001$]. The ANOVAs showed no significant main effect of group for the intensity ratings [$F(1,28) = .70$, $p = .411$] or for the reaction times [$F(1,28) = 1.749$, $p = .197$] and no significant interaction between group and condition [$F(1,28) = .39$, $p = .539$ and $F(1,28) = .92$, $p = .347$, respectively].

3.3. Eye-movement data

To ensure that differential gaze patterns did not confound any of our results, we first analyzed eye-movement data as to whether healthy controls and JME patients differed in the way they looked at the stimuli. Overall, gaze behavior differed between the two stimulus conditions as indicated by longer durations of the fixations in the painful condition [$M_{neutral} = 297.96$ msec, $SD_{neutral} = 45.00$ msec, $M_{painful} = 348.17$ msec, $SD_{painful} = 66.07$ msec, $F(1,23) = 52.91$, $p < .001$] and the centrality of the fixation, which was closer to the center of the image [$M_{neural} = 96.23$ pxs, $SD_{neutral} = 17.56$ pxs, $M_{painful} = 83.26$ pxs, $SD_{painful} = 21.17$ pxs, $F(1,23) = 21.75$, $p < .001$, Fig. 1B]. At the same time the average frequency of fixations per image presentation was reduced, which was related to the longer fixation duration and reduced image exploration in the painful condition [$M_{neutral} = 11.17$, $SD_{neutral} = 1.68$, $M_{painful} = 9.60$, $SD_{painful} = 1.86$, $F(1,23) = 76.97$, $p < .001$] overall indicating greater attention to the painfully stimulated limbs. Importantly, we found no significant group differences [$Fs(1,23) < .125$, all $ps > .727$] and no significant interaction between GROUP and CONDITION [$Fs(1,23) < 1.43$, all $ps > .243$] for any of these measures. Hence, any difference between patients in controls cannot be explained by differences in gaze behavior.

3.4. Pupil dilation data

After an initial constriction of about 400 msec, participants' pupil continued to dilate until 1.7 sec after stimulus onset (Fig. 1D). While for neutral pictures the pupil size plateaued afterwards, for painful pictures dilation continued the end of the stimulus presentation. The 'pupil slope' indicated a significant main effect of condition [$F(1,23) = 95.12$, $p < .001$, $\eta^2 = .81$, rmANOVA] and a significant interaction between group and condition [$F(1,23) = 7.82$, $p = .01$, $\eta^2 = .25$], which remained statistically significant after controlling for potential trend level differences ($p = .079$, Table 1) in the participants' verbal IQ [$F(1,22) = 8.13$, $p = .009$, $\eta^2 = .27$]. Notably, the interaction effect in the pupil dilation also survived corrections for multiple-comparisons. Considering the four pain empathy related dependent variables, alexithymia, intensity ratings, reaction times, and the pupil slope, the significance of the effect is still below the Bonferroni corrected alpha-level of $p = .0125$ ($p = .05/4 = .0125$ *vs* $p = .0102$). Further, the interaction between group and condition remained significant after controlling for each treatment with either lamotrigine [$F(1,22) = 4.58$, $p = .04$], levetiracetam [$F(1,22) = 6.84$, $p = .02$], or valproate [$F(1,22) = 6.62$, $p = .02$]. The main effect of group was not significant [$F(1,23) = 1.51$, $p = .232$].

Post-hoc comparisons indicated that the main effect of condition resulted from larger pupil slopes in response to painful pictures ($M = 1.10$, $SD = .51$) as compared to neutral pictures [$M = .60$, $SD = .48$, $t(24) = 8.71$, $p < .001$]. The significant interaction between group and condition was explained by comparable pupil slopes of the control group ($M = .65$, $SD = .49$) and the JME group [$M = .56$, $SD = .49$, $t(23) = .45$, $p = .327$] in response to neutral pictures, but a significantly stronger sustained pupil dilation in controls ($M = 1.28$, $SD = .36$) compared to JME patients [$M = .91$, $SD = .58$, $t(23) = 1.94$, $p < .033$, corrected for non-sphericity] in response to painful pictures. Importantly, none of the group differences could be attributed to how subjects looked at the images, as none of the obtained measures of gaze behavior showed any indication of differences in image exploration between groups.

3.5. Neuroimaging data

The task induced a pattern of cortical activity very typical for pain empathy in response to observing pictures of painful stimulation of another's limbs (Lamm, Decety, & Singer, 2011). The average effect of viewing painful pictures in comparison to neutral pictures ([JME_pain − JME_neutral] + [HC_pain-HC_neutral]) indicated several clusters within the ACC/MCC, the bilateral AI, primary and higher-order somatosensory cortex areas in Brodmann Area (BA) 1 and BA 2 as well as the inferior parietal lobe, and the ventrolateral prefrontal cortex

(VLPFC) to be involved in empathy for pain ($p < .05$, corrected, Table 3). Within this network, however, the JME patients showed significantly less empathy for pain-related activation compared to the matched controls ([HC_pain – HC_neutral] – [JME_pain – JME_neutral]). ROI analyses indicated reduced sensitivity to another person's pain in the ACC/MCC cluster [6, 20, 38 mm, $t(28) = 3.51$, $p = .041$, corrected], the right AI [30, 28, 4 mm, $t(28) = 3.29$, $p = .026$, corrected], and the VLPFC [−48, 44, 2 mm, $t(28) = 4.40$, $p = .002$, corrected, see Table 3 and Fig. 2A,B]. These effects remained significant after controlling for participants' verbal IQ ($ps < .044$, corrected). Within the left AI we observed a similar effect, which however was significant only at an uncorrected trend level [−40, 18, 6 mm, $t(28) = 3.04$, $p = .136$, corrected, corresponding to $p = .003$, uncorrected].

To examine common variance of pupil dilation and hemodynamic responses, we computed the conjunction of the average effect of the parametric weights of the pupil dilation across both groups ([JME_pain + JME_neutral]∩[HC_pain + HC_neutral]). Significant and consistent associations of the pupil slope with the hemodynamic response were found within the task-activated network and subcortical regions. The ROI analyses within the task-activated network revealed significant association of the pupil slope with the hemodynamic signal in the ACC/MCC cluster [6, 20, 42 mm, $t(44) = 4.55$, $p < .002$, corrected], the left AI [−32, 24, −2 mm, $t(44) = 3.72$, $p < .022$, corrected], and the right AI [−38, 24, 4 mm, $t(44) = 3.21$, $p < .023$, corrected, see Table 4, Fig. 2C,D and Fig. 1C for an illustration of the effects on the within-subject level]. Further, the whole-brain analysis indicated a cluster within the bilateral thalamus to survive the cluster extent threshold at $p = .041$ [corresponding to $t(44) > 2.69$, $p < .005$, $k = 630$; right thalamus at 6, −8, 10 mm, $t(44) = 3.84$ and left thalamus −8, −6, 10 mm, $t(44) = 3.62$].

On average, the pattern of the functional integration of the ACC showed considerable overlap with the task-activated network and strongest signal correlations with the bilateral ACCs were found in the AIs, VLPFCs, and bilateral somatosensory cortex areas. In JME patients, the whole-brain analysis revealed a significantly decreased coupling of the right ACC with primary and higher-order somatosensory cortex areas in the right hemisphere. After controlling for the influences of task-induced hemodynamics and noise due to head movement or global signal fluctuations, compared to controls, the right ACC in JME patients showed lower signal correspondence with a cluster covering BA 1 at 64, −12, 28 mm, BA 3b at 40, −26, 44 mm and the parietal operculum at 60, −10, 12 mm [$p = .047$, corrected, corresponding to $p < .005$, uncorrected, $t(28) > 2.76$, $k = 611$, Table 5 and Fig. 3]. A similar and in part overlapping cluster was observed for the left ACC, showing a reduced functional connectivity with the right somatosensory cortex in BA 2 at 44, −28, 56 mm, and BA 3b at 28, −42, 60 mm, at trend level [$p = .064$, corrected, corresponding to $p < .005$, uncorrected, $t(28) > 2.76$, $k = 492$]. Besides these findings, within the present sample we also found partial support for previous evidence (Vollmar et al., 2012) indicating reduced connectivity of the left ACC with SMA regions in the left hemisphere at 10, −18, 58 mm [$p = .124$, corrected, corresponding to $p < .005$, uncorrected, $t(28) > 2.76$, $k = 406$].

Table 3 – Group differences and empathy for pain-associated activation.

Brain region	Cyto area	Side	Cluster size	MNI coordinates			T	pFWE
				x	y	z		
Pain > No pain								
Anterior cingulate		R/L	1149	−4	20	42	10.74	<.001
				−4	28	40	10.06	<.001
				−8	30	28	7.43	.002
Anterior insula		L	1122	−40	18	6	9.81	<.001
				−46	14	−6	8.41	<.001
	Area 44			−52	6	14	8.00	.001
Anterior insula		R	189	48	14	4	8.70	<.001
	Area 44			54	12	12	7.12	.003
Anterior insula		R	98	28	22	6	7.89	.001
				38	20	0	6.10	.032
Somatosensory	IPC(PFop)	L	598	−58	−22	24	8.84	<.001
	IPC(PFt)			−58	−26	34	8.50	<.001
	Area 1			−44	−30	62	7.74	.001
Somatosensory	Area 2	R	95	62	−22	44	8.60	<.001
	IPC(PFt)			48	−28	44	7.21	.003
Ventrolateral prefrontal		L	113	−48	44	4	8.94	<.001
Putamen		L	31	−14	10	2	6.94	.005
Putamen		R	15	14	12	0	6.47	.014
Control > JME × Pain > No pain								
Anterior cingulate		R	218	6	20	38	3.51	.041
Anterior insula		R	39	30	28	4	3.29	.026
Ventrolateral prefrontal		L	44	−48	44	2	4.40	.002

Note. All statistics for the average effect of Pain > No Pain are thresholded at $p < .05$, familywise error (FWE) corrected for a whole-brain analysis, $k > 10$. The interaction effect was examined in the activated regions of interests (ROIs) and p values were corrected within the respective ROI. The cluster extend of the ROI analyses refers to the $p < .05$ uncorrected cluster size within each ROI. The 'Cyto Area' column indicates the assigned cytoarchitectonic area as indicated by the SPM ANATOMY toolbox v1.8 if available.

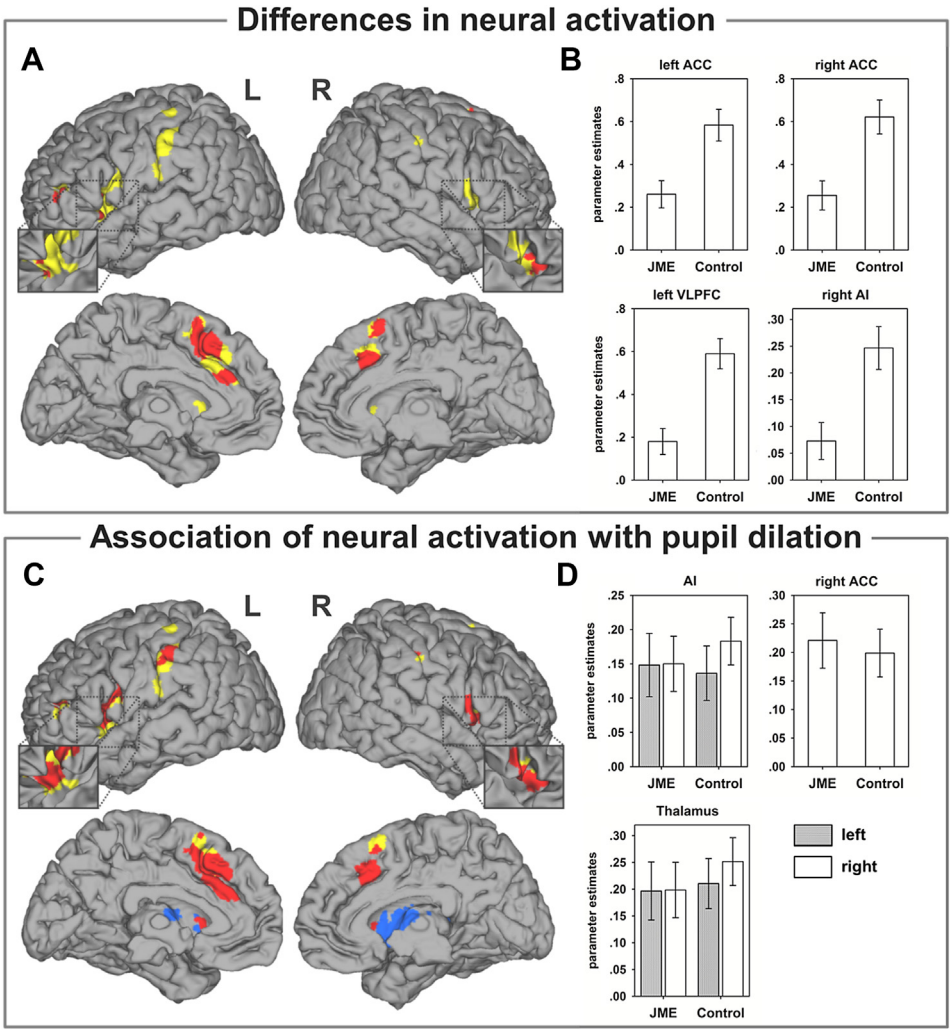

Fig. 2 – Reduced activation of the JME group within the task-activated network and association of pupil dilation with hemodynamic responses. A Brain areas showing reduced activation in JME patients (red) compared to healthy controls (HC) within the empathy for pain-related activation (yellow) rendered on an individual surface image. For display purposes, the results of the interaction of group and condition ([HC_pain – HC_neutral] – [JME_pain – JME_neutral]) were thresholded at $t(28) > 1.70$, $p < .05$, uncorrected, and were masked by the task-activated network ([JME_pain – JME_neutral] + [HC_pain – HC_neutral]), which was thresholded at $t(28) > 5.89$, $p < .05$, corrected. B Parameter estimates of clusters that show significant reduction of empathy for pain-related activation in the JME group at corrected thresholds. Parameter estimates are plotted together with standard errors at the peak voxel and illustrate the contrast of Pain-Neutral for each group within the left and right anterior cingulate cortex (ACC), the right anterior insula (AI), and the left ventrolateral prefrontal cortex (VLPFC). C Brain areas where the hemodynamic signal is positively associated with the 'pupil slope' rendered on an individual surface image. Clusters within the empathy for pain-related network (yellow) are coded in red while areas outside the network are coded in blue. The conjunction analysis of the parametric weights of the pupil slope in both groups ([JME_pain + JME_neutral]∩[HC_pain + HC_neutral]) was thresholded at $t(44) > 2.69$, $p < .005$, uncorrected, and plotted together with the task-activated network ([JME_pain – JME_neutral] + [HC_pain – HC_neutral]), which was thresholded at $t(28) > 5.89$, $p < .05$, corrected, for displaying purposes. D Parameter estimates of the clusters that show significant association of sustained pupil dilation with hemodynamic responses consistently across both groups. Parameter estimates are plotted together with standard errors at the peak voxel and illustrate the average effect of the conditions (0.5×[pain + neutral]) for each group within the bilateral AI, the right ACC, and the bilateral thalamus.

4. Discussion

In this study we used the specific psychopathology associated with JME to directly test the role of the mesial fronto-insular network for social adjustment in patients and healthy controls. Although the peculiarities in the personality structure of JME patients have been related to structural abnormalities in the mesial-frontal lobe and dysfunctions of fronto-thalamical

Table 4 – Positive association of hemodynamic responses with variability in the slope of the pupil dilation.

Brain region	Cyto area	Side	Cluster size	MNI coordinates			T	pFWE
				x	y	z		
Cluster extend threshold								
Thalamus	Th-Temporal	R	630	6	−8	10	3.84	.041
	Th-Temporal	L		−8	−6	10	3.62	
		R		10	6	−2	3.60	
	Th-Prefrontal	L		−12	−18	12	3.06	
ROI analyses								
Anterior cingulate		R	117	6	20	42	4.55	.002
Anterior insula		L	142	−32	24	−2	3.72	.022
Anterior insula		R	9	38	24	4	3.21	.023
		R	5	28	20	6	3.09	.030

Note. FWE = Familywise error correction for the respective peak voxel in case of the region of interest (ROI) analysis or cluster extent in case of the whole-brain analysis. Effects represent the average effect of the parametric weights for the Neutral and Pain condition in a conjunction across the JME and Control group. All cluster extends refer to $p < .005$, uncorrected. ROIs were similar to those used for examining activation differences between the JME and Control groups. The 'Cyto Area' column indicates the assigned cytoarchitectonic area as indicated by the SPM ANATOMY toolbox v1.8 if available.

circuits earlier, this hypothesis had not been tested directly with respect to brain function in context of social paradigms. By assessing the physiological parameters while observing others' bodily pain by simultaneous pupillometry and fMRI, we verified the main hypothesis that JME impacts the empathy for pain response within mesial-frontal circuits. Within the task-activated network, patients with JME showed reduced empathy for pain-related responses in dorsal aspects of the ACC, the right AI, and the left VLPFC. These data were supported by less-pronounced pupil dilation to painful stimuli in the JME group, which was linked to the neural activity in the bilateral ACC, the AI, and the thalamus on the within-subject level. The neural activation in brain systems that regulate homeostasis (Craig, 2009) thus directly translated to the observed pattern of the pupil response providing multi-modal evidence for altered pain empathy in patients with JME. The decreased connectivity of primary and higher-order somatosensory cortex areas with the ACC, which are of particular importance for the somatic representations of another person's pain (Keysers et al., 2010), thereby characterizes a neural pathway that helps explaining the altered response of fronto-insular circuits and disturbances in psychosocial behavior.

Previous studies have mainly concentrated on structural abnormalities in JME patients on a micro (Meencke, 1985; Meencke & Janz, 1984) as well as macro level (Betting et al., 2006; Deppe et al., 2008; Kim et al., 2007; O'Muircheartaigh et al., 2012; Woermann et al., 1999), while mesial-frontal brain functioning was only examined in the context of cognitive paradigms such as working memory (Vollmar et al., 2011) or word generation (O'Muircheartaigh et al., 2012). These studies characterized atypical interactions of higher motor systems with cortical and subcortical structures, providing insights into how cognitive effort related to the specific JME psychopathology. Especially the SMA and pre-SMA have thus been considered central hub regions in the pathological architecture of the neural system's functioning

Table 5 – Reduced functional connectivity of the bilateral ACC in JME patients.

Brain region	Cyto area	Side	Cluster size	MNI coordinates			T	pFWE
				x	y	z		
Functional connectivity of the right anterior cingulate cortex								
Somatosensory	IPC(PF)	R	611	66	−26	34	4.98	.047
	OP4	R		60	−10	12	3.78	
	Area 1	R		64	−12	28	3.78	
	Area 1	R		38	−36	62	3.50	
	Area 3b	R		40	−26	44	3.34	
Functional connectivity of the left anterior cingulate cortex								
Somatosensory	Area 3b	R	492	44	−28	56	4.36	.064
	Area 3b	R		34	−38	58	4.24	
	Area 2	R		28	−42	60	4.23	
	Area 4a	R		38	−22	56	3.58	
SMA/Somatosensory	Area 2	L	406	−36	−40	58	3.65	.127
	Area 4p	L		−14	−30	60	3.36	
	Area 6	L		10	−18	58	3.33	

Note. FWE = Familywise error correction for the respective cluster extent. All cluster sizes refer to $p < .005$, uncorrected, and are reported for clusters exceeding $k > 400$. The 'Cyto Area' column indicates the assigned cytoarchitectonic area as indicated by the SPM ANATOMY toolbox v1.8 if available.

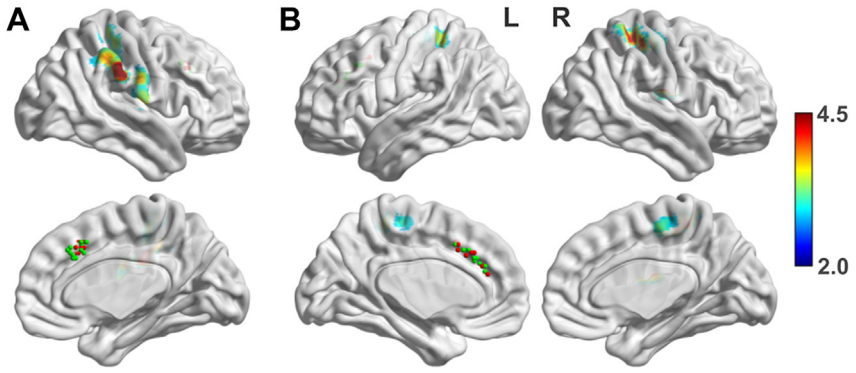

Fig. 3 – Reduced functional connectivity of the bilateral ACCs with somatosensory cortex areas and the supplementary motor area in JME patients. A Brain areas with significantly reduced connectivity of the right ACC in JME patients rendered on the right hemisphere of the ICBM 152 brain surface in MNI space. The depicted cluster survived the family-wise error correction of the cluster extent threshold in the whole-brain analysis at $p < .047$. Cytoarchitectonic references indicated maxima at primary and higher-order somatosensory cortex areas in Area 1, Area 3b, and the parietal operculum. B At trend level, the left ACC also had reduced connectivity with the somatosensory cortex in Area 2 and Area 3b ($p = .064$, corrected) as well as the supplementary motor area in the medial Area 6. All render images were thresholded at $t(28) > 2.76$, $p < .005$, $k > 400$ and include the location of the left or right hemispheric seed time series for JME patients (green) and healthy controls (red).

(Vollmar et al., 2012), potentially helping to also understand emotional instabilities and difficulties in socio-emotional adjustment. Given the frequent comorbidities with psychiatric conditions, however, this indirect evidence might not suffice to understand the complex psychopathology of JME patients. Instead, the present findings suggest that dysfunctions in the social domain could be explained via altered responses of the ACC and AI network and reduced functional integration between primary and higher-order somatosensory cortex areas and the ACC. This is supported by a considerable body of literature that ascribes the ACC and AI a crucial role in the understanding and regulation of one's own emotions (Berthoz et al., 2002; Craig, 2009; Damasio et al., 2000; Eippert et al., 2007) and altered functioning, specifically of the AI, in alexithymia (Bernhardt et al., 2013; Bird et al., 2010). Beyond empathy for physical pain, this network thus also has strong implications in the experience of other social emotions such as sharing happiness (Jabbi & Keysers, 2008; Mobbs et al., 2009), disgust (Jabbi, Bastiaansen, & Keysers, 2008; Wicker et al., 2003) or social pain (Krach et al., 2011; Paulus, Müller-Pinzler, et al., 2014) with significant consequences for interpersonal behavior: the fMRI response pattern observed herein to be altered in JME patients, had previously been described motivating helping behavior in healthy observers (Hein et al., 2010; Masten, Morelli, & Eisenberger, 2011) and related to disorders that are characterized by impairments in social interactions (Masten, Colich, et al., 2011; Masten, Morelli, et al., 2011; Meffert et al., 2013; Silani et al., 2008). In accordance with the previous evidence for patients with epilepsy in the ACC to have difficulties in social adjustment (Devinsky, Morrell, & Vogt, 1995), the present findings corroborate the notion that dysfunctions within the ACC circuits might mediate disturbances in social behavior, also in JME patients. This study thus is the first to demonstrate that the peculiarities in the personality structure, including emotional instability, rapid mood changes or difficulties in social adjustment and the increased probability of comorbid psychiatric conditions in JME, may not solely be attributed to the side effects of the dysexecutive syndrome; instead, our data suggest that they result from alterations in neural circuits that are directly involved in regulating affect.

It is unknown whether our findings result from generalized alterations in the ACC's functioning during emotion processing or whether the reduced reactivity is specific to impairments in empathizing with another. Even though recent fMRI studies showed similar involvement of the ACC, AI, and the VLPFC in pain empathy and the pain experienced on one's own body, both have to be considered as conceptually and psychologically distinct phenomena (Keysers & Gazzola, 2007). The psychopathology of JME, specifically the emotional instability (Gelisse et al., 2007) and the here described trend for higher levels in alexithymia, might nonetheless suggest the reduced pain-empathy response to be driven by rather general alterations in the affective response of the ACC and AI network and reduced integration of information from somatosensory cortex areas in mesial-frontal circuits. The present findings of altered frontal functioning during empathy for pain thus might have the potential to also generalize to first-person experiences of pain and explain the often observed difficulties of JME patients in the experience and regulation of affect (De Araujo Filho et al., 2013). However, future studies need to directly address the role of the ACC's and the AI's functioning in first-person experiences of negative affect in order to understand their contribution to the JME psychopathology more comprehensively.

The present findings also provide new insight in the link of pupil dynamics with neural systems activity during emotional processing. While changes in pupil diameter occur in response to diverse stimulus features and psychological

processes (Preuschoff, 2011; Steinhauer et al., 2004), the current pattern of continuous pupil dilation during stimulus presentation has also been previously related to processing negative emotions (Bradley et al., 2008) and the experience of pain on one's own body (Geuter et al., 2014). The physiology of this characteristic pupil response to emotional stimuli has been explained by activity of the sympathetic system that innervates the iris dilator, resulting in the observed increase of the pupil's size. The involvement of the sympathetic system in pupil dilation during emotional processing is empirically supported by close covariation of pupil diameter with skin conductance responses (Bradley et al., 2008) and the predictive value of the magnitude of pupil dilation for the intensity of the experienced affect (Geuter et al., 2014). The now described association of pupil dilation with ACC and AI activation, brain systems that have strong implications in the regulation of homeostasis, is in line with previous work that indicated a very similar coupling of increase in pupil size with autonomic activity and stress-induced activation of the ACC (Critchley, Tang, Glaser, Butterworth, & Dolan, 2005). The link of neural activity in neural systems that process emotional arousal with a specific and characteristic pattern observable pupil dynamics thus opens up new perspectives for non-invasive investigations of affective responses in more complex social scenarios that require ecological plausible environments, which are difficult to realize in the fMRI setting (Krach, Müller-Pinzler, Westermann, & Paulus, 2013).

Notably, the reduced pupil dilation in the JME sample could not be explained by the antiepileptic medication. While a more recent case report suggested *lamotrigine* to affect eye movements in children (Das, Harris, Smyth, & Cross, 2003), an earlier study with a larger sample of healthy volunteers found no evidence for this effect (Hamilton et al., 1993) and instead related *carbamazepine* to alterations in smooth and saccadic eye movements. Importantly, this study found no effects on pupil dynamics and neither did another study for valproate (DeMet & Sokolski, 1999). Hence there is no prior data suggesting an effect of antiepileptic drugs on pupils' response, which was also supported with the present data; after including the anticonvulsant medications as nuisance regressors, the significance of the effects remained unchanged.

In conclusion, the present study provides further evidence for the neural basis of specific aspects of JME patients' psychopathology. Consistent with our predictions, the fMRI data indicated less-pronounced neural responses in the frontal circuits that mediate the empathic sharing of unpleasant feelings. This was paralleled by similar effects observed for pupil dilation, which we link to neural activity in brain systems with strong implications in homeostatic regulation. The correlation of the pupils' reactivity with neural activation within the ACC, thalamic, and insular network represents the first combined evidence for reduced physiological reactivity of patients with JME in response to social stimuli which could be explained by reduced functional interaction among somatosensory cortex areas and the ACC. This multi-modal approach thus helps to better understand the complex clinical picture of JME patients by explaining the peculiarities in psychosocial behavior with disturbances in mesial-frontal circuits, and contributes to a better understanding of the neural foundations of social behavior in general.

Acknowledgments

This work was supported by research grants from the 'Deutsche Forschungsgemeinschaft' (DFG grant no. KR3803/2-1, KR3803/7-1 and EI852/3-1), the 'Landes-Offensive zur Entwicklung Wissenschaftlich-ökonomischer Exzellenz (LOEWE)', and the 'Research Foundation of the University of Marburg'. The authors would also like to thank Rita Werner and Jens Sonntag for their assistance during data collection and one anonymous reviewer who helped to improve the quality of the manuscript.

REFERENCES

Bernhardt, B. C., Valk, S. L., Silani, G., Bird, G., Frith, U., & Singer, T. (2013). Selective disruption of sociocognitive structural brain networks in autism and alexithymia. *Cerebral Cortex*. http://dx.doi.org/10.1093/cercor/bht182.

Berthoz, S., Artiges, E., Van De Moortele, P.-F., Poline, J.-B., Rouquette, S., Consoli, S. M., et al. (2002). Effect of impaired recognition and expression of emotions on frontocingulate cortices: an fMRI study of men with alexithymia. *The American Journal of Psychiatry, 159*(6), 961–967.

Betting, L. E., Mory, S. B., Li, L. M., Lopes-Cendes, I., Guerreiro, M. M., Guerreiro, C. A. M., et al. (2006). Voxel-based morphometry in patients with idiopathic generalized epilepsies. *NeuroImage, 32*(2), 498–502. http://dx.doi.org/10.1016/j.neuroimage.2006.04.174.

Bird, G., Silani, G., Brindley, R., White, S., Frith, U., & Singer, T. (2010). Empathic brain responses in insula are modulated by levels of alexithymia but not autism. *Brain, 133*(Pt 5), 1515–1525. http://dx.doi.org/10.1093/brain/awq060. awq060 [pii].

Bradley, M. M., Miccoli, L., Escrig, M. A., & Lang, P. J. (2008). The pupil as a measure of emotional arousal and autonomic activation. *Psychophysiology, 45*(4), 602–607. http://dx.doi.org/10.1111/j.1469-8986.2008.00654.x.

Brett, M., Anton, J.-L., Valabregue, R., & Jean-Baptiste, P. (2002). Region of interest analysis using an SPM toolbox. In *8th International Conference on Functional Mapping of the Human Brain*.

Cox, B. J., Swinson, R. P., Shulman, I. D., & Bourdeau, D. (1995). Alexithymia in panic disorder and social phobia. *Comprehensive Psychiatry, 36*(3), 195–198. http://dx.doi.org/10.1016/0010-440X(95)90081-6.

Craig, A. D. (2009). How do you feel–now? The anterior insula and human awareness. *Nature Reviews Neuroscience, 10*(1), 59–70. http://dx.doi.org/10.1038/nrn2555.

Critchley, H. D., Tang, J., Glaser, D., Butterworth, B., & Dolan, R. J. (2005). Anterior cingulate activity during error and autonomic response. *NeuroImage, 27*(4), 885–895. http://dx.doi.org/10.1016/j.neuroimage.2005.05.047.

Damasio, A. R., Grabowski, T. J., Bechara, A., Damasio, H., Ponto, L. L., Parvizi, J., et al. (2000). Subcortical and cortical brain activity during the feeling of self-generated emotions. *Nature Neuroscience, 3*(10), 1049–1056. http://dx.doi.org/10.1038/79871.

Das, K. B., Harris, C., Smyth, D. P. L., & Cross, J. H. (2003). Unusual side effects of lamotrigine therapy. *Journal of Child Neurology, 18*(7), 479–480. http://dx.doi.org/10.1177/08830738030180070301.

Davis, M. H. (1996). *Empathy: A social-psychological approach*. Boulder: Westview Press.

De Araujo Filho, G. M., de Araujo, T. B., Sato, J. R., Silva, I., Da, Lin, K., Júnior, H. C., et al. (2013). Personality traits in juvenile myoclonic epilepsy: evidence of cortical abnormalities from a

surface morphometry study. *Epilepsy & Behavior: E&B, 27*(2), 385–392. http://dx.doi.org/10.1016/j.yebeh.2013.02.004.
DeMet, E. M., & Sokolski, K. N. (1999). Sodium valproate increases pupillary responsiveness to a cholinergic agonist in responders with mania. *Biological Psychiatry, 46*(3), 432–436.
Deppe, M., Kellinghaus, C., Duning, T., Möddel, G., Mohammadi, S., Deppe, K., et al. (2008). Nerve fiber impairment of anterior thalamocortical circuitry in juvenile myclonic epilepsy. *Neurology, 71*(24), 1981–1985. http://dx.doi.org/10.1212/01.wnl.0000336969.98241.17.
Devinsky, O., Morrell, M. J., & Vogt, B. A. (1995). Contributions of anterior cingulate cortex to behaviour. *Brain, 118*, 279–306.
Eickhoff, S. B., Stephan, K. E., Mohlberg, H., Grefkes, C., Fink, G. R., Amunts, K., et al. (2005). A new SPM toolbox for combining probabilistic cytoarchitectonic maps and functional imaging data. *NeuroImage, 25*(4), 1325–1335. http://dx.doi.org/10.1016/j.neuroimage.2004.12.034. S1053-8119(04)00792-X [pii].
Eippert, F., Veit, R., Weiskopf, N., Erb, M., Birbaumer, N., & Anders, S. (2007). Regulation of emotional responses elicited by threat-related stimuli. *Human Brain Mapping, 28*(5), 409–423. http://dx.doi.org/10.1002/hbm.20291.
Esslinger, C., Walter, H., Kirsch, P., Erk, S., Schnell, K., Arnold, C., et al. (2009). Neural mechanisms of a genome-wide supported psychosis variant. *Science, 324*(5927), 605. http://dx.doi.org/10.1126/science.1167768, 324/5927/605 [pii].
Gelisse, P., Thomas, P., Samuelian, J. C., & Gentin, P. (2007). Psychiatric disorders in juvenile myoclonic epilepsy. *Epilepsia, 48*(5), 1032–1033. http://dx.doi.org/10.1111/j.1528-1167.2007.01009_4.x. EPI1009_4 [pii].
Geuter, S., Gamer, M., Onat, S., & Büchel, C. (2014). Parametric trial-by-trial prediction of pain by easily available physiological measures. *Pain, 155*(5), 994–1001. http://dx.doi.org/10.1016/j.pain.2014.02.005.
Hamilton, M. J., Cohen, A. F., Yuen, A. W. C., Harkin, N., Land, G., Weatherley, B. C., et al. (1993). Carbamazepine and lamotrigine in healthy volunteers: relevance to early tolerance and clinical trial dosage. *Epilepsia, 34*(1), 166–173. http://dx.doi.org/10.1111/j.1528-1157.1993.tb02393.x.
Hein, G., Silani, G., Preuschoff, K., Batson, C. D., & Singer, T. (2010). Neural responses to ingroup and outgroup members' suffering predict individual differences in costly helping. *Neuron, 68*(1), 149–160. http://dx.doi.org/10.1016/j.neuron.2010.09.003. S0896-6273(10)00720-8 [pii].
Holmes, M. D., Quiring, J., & Tucker, D. M. (2010). Evidence that juvenile myoclonic epilepsy is a disorder of frontotemporal corticothalamic networks. *NeuroImage, 49*(1), 80–93. http://dx.doi.org/10.1016/j.neuroimage.2009.08.004.
Jabbi, M., Bastiaansen, J., & Keysers, C. (2008). A common anterior insula representation of disgust observation, experience and imagination shows divergent functional connectivity pathways. *PloS One, 3*(8), e2939. http://dx.doi.org/10.1371/journal.pone.0002939.
Jabbi, M., & Keysers, C. (2008). Inferior frontal gyrus activity triggers anterior insula response to emotional facial expressions. *Emotion, 8*(6), 775–780. http://dx.doi.org/10.1037/a0014194.
Jackson, P. L., Meltzoff, A. N., & Decety, J. (2005). How do we perceive the pain of others? A window into the neural processes involved in empathy. *NeuroImage, 24*(3), 771–779. http://dx.doi.org/10.1016/j.neuroimage.2004.09.006.
Janisse, M. P. (1974). Pupil size, affect and exposure frequency. *Social Behavior and Personality, 2*(2), 125–146. http://dx.doi.org/10.2224/sbp.1974.2.2.125.
Janz, D. (1985). Epilepsy with impulsive petit mal (juvenile myoclonic epilepsy). *Acta Neurologica Scandinavica, 72*(5), 449–459.
Janz, D., & Christian, W. (1957). Impulsiv-Petit mal. *Deutsche Zeitschrift Für Nervenheilkunde, 176*(3), 346–386. http://dx.doi.org/10.1007/BF00242439.
Keysers, C., & Gazzola, V. (2007). Integrating simulation and theory of mind: from self to social cognition. *Trends in Cognitive Sciences, 11*(5), 194–196. http://dx.doi.org/10.1016/j.tics.2007.02.002.
Keysers, C., Kaas, J. H., & Gazzola, V. (2010). Somatosensation in social perception. *Nature Reviews Neuroscience, 11*(6), 417–428. http://dx.doi.org/10.1038/nrn2833.
Kim, J. H., Lee, J. K., Koh, S.-B., Lee, S.-A., Lee, J.-M., Kim, S. I., et al. (2007). Regional grey matter abnormalities in juvenile myoclonic epilepsy: a voxel-based morphometry study. *NeuroImage, 37*(4), 1132–1137. http://dx.doi.org/10.1016/j.neuroimage.2007.06.025.
Krach, S., Cohrs, J. C., de Echeverria Loebell, N. C., Kircher, T., Sommer, J., Jansen, A., et al. (2011). Your flaws are my pain: linking empathy to vicarious embarrassment. *PloS One, 6*(4), e18675. http://dx.doi.org/10.1371/journal.pone.0018675.
Krach, S., Müller-Pinzler, L., Westermann, S., & Paulus, F. M. (2013). Advancing the neuroscience of social emotions with social immersion. *The Behavioral and Brain Sciences, 36*(4), 427–428. http://dx.doi.org/10.1017/S0140525X12001951.
Lamm, C., Decety, J., & Singer, T. (2011). Meta-analytic evidence for common and distinct neural networks associated with directly experienced pain and empathy for pain. *NeuroImage, 54*(3), 2492–2502. http://dx.doi.org/10.1016/j.neuroimage.2010.10.014. S1053-8119(10)01306-6 [pii].
Lyon, G., & Gastaut, H. (1985). Considerations on the significance attributed to unusual cerebral histological findings recently described in eight patients with primary generalized epilepsy. *Epilepsia, 26*(4), 365–367. http://dx.doi.org/10.1111/j.1528-1157.1985.tb05664.x.
Masten, C. L., Colich, N. L., Rudie, J. D., Bookheimer, S. Y., Eisenberger, N. I., & Dapretto, M. (2011). An fMRI investigation of responses to peer rejection in adolescents with autism spectrum disorders. *Developmental Cognitive Neuroscience, 1*(3), 260–270. http://dx.doi.org/10.1016/j.dcn.2011.01.004.
Masten, C. L., Morelli, S. A., & Eisenberger, N. I. (2011). An fMRI investigation of empathy for "social pain" and subsequent prosocial behavior. *NeuroImage, 55*(1), 381–388. http://dx.doi.org/10.1016/j.neuroimage.2010.11.060. S1053-8119(10)01538-7 [pii].
Meencke, H. J. (1985). Neuron density in the molecular layer of the frontal cortex in primary generalized epilepsy. *Epilepsia, 26*(5), 450–454.
Meencke, H. J., & Janz, D. (1984). Neuropathological findings in primary generalized epilepsy: a study of eight cases. *Epilepsia, 25*(1), 8–21.
Meffert, H., Gazzola, V., den Boer, J. A., Bartels, A. A. J., & Keysers, C. (2013). Reduced spontaneous but relatively normal deliberate vicarious representations in psychopathy. *Brain, 136*(8), 2550–2562. http://dx.doi.org/10.1093/brain/awt190.
Mobbs, D., Yu, R., Meyer, M., Passamonti, L., Seymour, B., Calder, A. J., et al. (2009). A key role for similarity in vicarious reward. *Science, 324*(5929), 900. http://dx.doi.org/10.1126/science.1170539.
O'Muircheartaigh, J., Vollmar, C., Barker, G. J., Kumari, V., Symms, M. R., Thompson, P., et al. (2011). Focal structural changes and cognitive dysfunction in juvenile myoclonic epilepsy. *Neurology, 76*(1), 34–40. http://dx.doi.org/10.1212/WNL.0b013e318203e93d.
O'Muircheartaigh, J., Vollmar, C., Barker, G. J., Kumari, V., Symms, M. R., Thompson, P., et al. (2012). Abnormal thalamocortical structural and functional connectivity in juvenile myoclonic epilepsy. *Brain, 135*(Pt 12), 3635–3644. http://dx.doi.org/10.1093/brain/aws296.

Parker, J. D., Taylor, G. J., & Bagby, R. M. (2003). The 20-item Toronto alexithymia scale. *Journal of Psychosomatic Research, 55*(3), 269–275. http://dx.doi.org/10.1016/S0022-3999(02)00578-0.

Partala, T., & Surakka, V. (2003). Pupil size variation as an indication of affective processing. *International Journal of Human-Computer Studies, 59*(1–2), 185–198. http://dx.doi.org/10.1016/S1071-5819(03)00017-X.

Paulus, F. M., Bedenbender, J., Krach, S., Pyka, M., Krug, A., Sommer, J., et al. (2014a). Association of rs1006737 in CACNA1C with alterations in prefrontal activation and fronto-hippocampal connectivity. *Human Brain Mapping, 35*, 1190–1200. http://dx.doi.org/10.1002/hbm.22244.

Paulus, F. M., Krach, S., Bedenbender, J., Pyka, M., Sommer, J., Krug, A., et al. (2013). Partial support for ZNF804A genotype-dependent alterations in prefrontal connectivity. *Human Brain Mapping, 34*(2), 304–313. http://dx.doi.org/10.1002/hbm.21434.

Paulus, F. M., Müller-Pinzler, L., Jansen, A., Gazzola, V., & Krach, S. (2014b). Mentalizing and the role of the posterior superior temporal sulcus in sharing others' embarrassment. *Cerebral Cortex*. http://dx.doi.org/10.1093/cercor/bhu011.

Preuschoff, K. (2011). Pupil dilation signals surprise: evidence for noradrenaline's role in decision making. *Frontiers in Neuroscience, 5*(September), 1–12. http://dx.doi.org/10.3389/fnins.2011.00115.

Savic, I., Lekvall, A., Greitz, D., & Helms, G. (2000). MR spectroscopy shows reduced frontal lobe concentrations of N-acetyl aspartate in patients with juvenile myoclonic epilepsy. *Epilepsia, 41*(3), 290–296.

Silani, G., Bird, G., Brindley, R., Singer, T., Frith, C., & Frith, U. (2008). Levels of emotional awareness and autism: an fMRI study. *Social Neuroscience, 3*(2), 97–112. http://dx.doi.org/10.1080/17470910701577020.

Silk, J. S., Dahl, R. E., Ryan, N. D., Forbes, E. E., Axelson, D. A., Birmaher, B., et al. (2007). Pupillary reactivity to emotional information in child and adolescent depression: links to clinical and ecological measures. *The American Journal of Psychiatry, 164*(12), 1873–1880. http://dx.doi.org/10.1176/appi.ajp.2007.06111816.

Steinhauer, S. R., Siegle, G. J., Condray, R., & Pless, M. (2004). Sympathetic and parasympathetic innervation of pupillary dilation during sustained processing. *International Journal of Psychophysiology: Official Journal of the International Organization of Psychophysiology, 52*(1), 77–86. http://dx.doi.org/10.1016/j.ijpsycho.2003.12.005.

Stoll, J., Chatelle, C., Carter, O., Koch, C., Laureys, S., & Einhäuser, W. (2013). Pupil responses allow communication in locked-in syndrome patients. *Current Biology, 23*(15), R647–R648. http://dx.doi.org/10.1016/j.cub.2013.06.011.

Taylor, G. J. (1984). Alexithymia: concept, measurement, and implications for treatment. *The American Journal of Psychiatry, 141*(6), 725–732.

Taylor, G. J., Michael Bagby, R., & Parker, J. D. A. (1991). The alexithymia construct: a potential paradigm for psychosomatic medicine. *Psychosomatics, 32*(2), 153–164. http://dx.doi.org/10.1016/S0033-3182(91)72086-0.

Van Essen, D. C., Drury, H. A., Dickson, J., Harwell, J., Hanlon, D., & Anderson, C. H. (2001). An integrated software suite for surface-based analyses of cerebral cortex. *Journal of the American Medical Informatics Association, 8*(5), 443–459. http://dx.doi.org/10.1136/jamia.2001.0080443.

Vollmar, C., O'Muircheartaigh, J., Barker, G. J., Symms, M. R., Thompson, P., Kumari, V., et al. (2011). Motor system hyperconnectivity in juvenile myoclonic epilepsy: a cognitive functional magnetic resonance imaging study. *Brain, 134*(Pt 6), 1710–1719. awr098 [pii] 10.1093/brain/awr098.

Vollmar, C., O'Muircheartaigh, J., Symms, M. R., Barker, G. J., Thompson, P., Kumari, V., et al. (2012). Altered microstructural connectivity in juvenile myoclonic epilepsy: the missing link. *Neurology, 78*(20), 1555–1559. http://dx.doi.org/10.1212/WNL.0b013e3182563b44.

Vulliemoz, S., Vollmar, C., Koepp, M. J., Yogarajah, M., O'Muircheartaigh, J., Carmichael, D. W., et al. (2011). Connectivity of the supplementary motor area in juvenile myoclonic epilepsy and frontal lobe epilepsy. *Epilepsia, 52*(3), 507–514. http://dx.doi.org/10.1111/j.1528-1167.2010.02770.x.

Wicker, B., Keysers, C., Plailly, J., Royet, J. P., Gallese, V., & Rizzolatti, G. (2003). Both of us disgusted in my insula: the common neural basis of seeing and feeling disgust. *Neuron, 40*(3), 655–664. S0896627303006792 [pii].

Woermann, F. G., Free, S. L., Koepp, M. J., Sisodiya, S. M., & Duncan, J. S. (1999). Abnormal cerebral structure in juvenile myoclonic epilepsy demonstrated with voxel-based analysis of MRI. *Brain, 122*, 2101–2108.

Xia, M., Wang, J., & He, Y. (2013). BrainNet Viewer: a network visualization tool for human brain connectomics. *PloS One, 8*(7), e68910. http://dx.doi.org/10.1371/journal.pone.0068910.